Evaluation of the protective performance of hydrophobic coatings applied on carbon-fibre epoxy composites

Heather O'Connor, Denis P. Dowling

[1] School of Mechanical and Materials Engineering, University College Dublin, Belfield, Dublin 4, Ireland

*** Correspondence:** Email: heather.oconnor@ucdconnect.ie

Abstract

Carbon-fibre epoxy composites are widely used for high performance structural applications, where they are often exposed to harsh environments. The result of moisture ingress has been extensively studied, causing significant deterioration in the mechanical properties of these composites. This study evaluates the performance of five commercial hydrophobic coatings as protective layers, to inhibit moisture ingress into the composite. The coatings evaluated were: NeverWet, HydroBead, SHC, Aculon and LiquidGlass. These coatings were characterised and compared in terms of hydrophobicity, surface energy, roughness and chemical composition. This study also evaluated two atmospheric plasma pre-treatments as a means of enhancing the adhesion performance of these coatings. The pre-treatments involved the use of an air plasma for the activation of the epoxy, as well as the plasma deposition of a nanometre thick SiO_x interlayer coating. The durability and protective performance of the coatings, with and without the pre-treatments were then compared using an abrasion test as well as a water immersion study.

The use of both plasma pre-treatments was found to enhance the adhesion and the abrasion performance of four out of the five coatings. Of the coatings and pre-treatments investigated, the LiquidGlass in conjunction with an SiO_x coating interlayer was found to exhibit the highest abrasion resistance. This was followed by the composite which was plasma activated prior to the application of the Aculon coating. Only minor differences were observed when comparing the total moisture ingress (M%) of the epoxy, coated with the different hydrophobic layers. The composite coated with the Aculon and SiO_x interlayer exhibited the least amount of moisture ingress, at 0.90 %, compared to 1.08 % of the uncoated specimen. The shear strength of epoxy composite, coated with the LiquidGlass, NeverWet and the activated Aculon combination, were within the range of the uncoated specimens, therefore the moisture ingress was reversible upon heating and no permanent damage to the epoxy-fibre interface was

observed. It is concluded that, of the five coatings investigated, both the Aculon coating and LiquidGlass in combination with an SiO_x interlayer coating, exhibit the greatest potential as protective layers for carbon fibre epoxy composites.

Keywords: Hydrophobic coatings; Carbon-fibre epoxy composite; Atmospheric pressure plasma; Polymer composite pre-treatments

1. Introduction

Polymer matrix composites (PMC's) are used extensively due to their strength to weight ratio, corrosion resistance and fatigue behaviour [1]. Carbon-fibre epoxy is an example of a PMC which is widely applied, when strength and durability are crucial e.g. for aerospace and marine applications. Despite the clear advantages over their steel and metal counterparts, degradation from weathering is inevitable over long periods of time. A number of authors have investigated the different degradation mechanisms of carbon-fibre epoxy composites [2-5]. Zafar et al. [2] for example, studied the effect of long-term moisture exposure on carbon-fibre epoxy by immersing samples for up to 230 days in demineralised and sea water. They observed an overall decrease in mechanical and interfacial properties due to water ingress, with sea water conditions having the highest impact on mechanical properties. Kumar et al. [5] investigated the synergistic effects of UV exposure and moisture. UV radiation, moisture and thermal cycling were found to have significant adverse effects on the epoxy polymer matrix, leading to extensive erosion of the epoxy matrix.

Moisture ingress is reported to cause changes in the thermophysical, mechanical and chemical characteristics of the epoxy matrix, however, unlike glass and aramid fibres, carbon fibres do not absorb moisture and their properties remain unaffected [6]. The epoxy matrix can undergo plasticization and hydrolysis, lowering its glass transition temperature [7]. Plasticization is reversible upon desorption of moisture, while the hydrolysis of chemical bonds usually results in more permanent irreversible damage to the epoxy. Overall, it has been concluded that matrix dominated properties, such as interlaminar strength and impact tolerance decrease significantly with moisture ingress [5].

Gelcoats, often poly or vinyl ester and polyurethanes have been traditionally applied to fibre reinforced polymer composites, for the required surface finish and as protective layers [8]. These coatings are normally applied as a paint [9], by electrostatic deposition of a powder or sprayed [10] or during an in-mould step, onto the cured composite laminates [11]. Extensive research has been conducted on how to improve the durability of protective gelcoat layers [12], particularly in terms of abrasive wear [13], moisture diffusion [14] and weather resistance [15].

Hydrophobic and superhydrophobic coatings exhibit water repellent properties and have found use in a broad range of applications, such as self-cleaning coatings [16], drag reduction [17], anti-icing [18] and biomedical [19]. The focus of this study is to carry out a comparison on the performance of commercial hydrophobic coatings to prevent moisture ingress into fibre reinforced composites. The five coatings, evaluated in this study were NeverWet [20], HydroBead [21], SHC, Aculon [22] and LiquidGlass [23]. While a small number of previous studies, have investigated the performance of some of these coatings individually[24], the objective in this study is to provide a coating comparison study. Some studies reported on novel coating technologies, using the NeverWet, HydroBead and Aculon coatings as the commercial reference coating [25-28]. These studies demonstrated that the presented laboratory scale coatings had enhanced abrasion resistance in comparison to commercial coatings [29, 30]. The commercial coating technologies available are often limited by the strength of the bonding between the substrate and the coating [30]. A further objective of the current study is to investigate the use of atmospheric pressure plasma treatments as a mechanism of enhancing coating adhesion.

Plasma activation of polymer surfaces, etches the surface and removes unwanted material, while producing new functional groups and crosslinking, which enhances the surface energy and the wettability of the material [31]. Plasmas can also be used to deposit coatings by polymerisation of monomers, which are passed through the discharge [32]. This creates a coating consisting of complicated, fragmented and rearranged units from the monomer, due to exposure to radicals and ions in the discharge [33]. In this study, in order to enhance the bonding of the commercial coatings, an atmospheric plasma jet is investigated as a pre-treatment through activation of the epoxy substrate, prior to the application of the hydrophobic coatings. Silicon oxide (SiO_x) rich interlayers, deposited using the same system were also evaluated as coating pre-treatments on the epoxy surface.

2. Experimental methods

2.1 Coatings and coating deposition

The five commercial hydrophobic coatings evaluated were NeverWet®, HydroBead®, SHC, Aculon© and NP's LiquidGlass. Rust Oleum's NeverWet coating is a low cost, two-part coating technology, specifically designed to create a moisture repelling barrier on a wide range of substrates, including metals, plastics and ceramics [20]. Siloxane derived nanoparticles are suspended in a hydrophobic solution and when deposited, form randomly distributed surface roughness features along the surface [24]. HydroBead's one-part water repelling aerosol coating, is reported by the manufacturer to protect against corrosion and ice-formation hydrobead [21]. The coating comprises of proprietary nanoparticles, suspended in a hydrophobic solution, forming a rough, low surface energy layer once deposited. The

third commercial coating, which cannot be named for proprietary reasons and is referred to as SHC (super hydrophobic coating). This coating contains undisclosed additives, suspended in an alcohol mixture, that upon evaporation, deposits a coating of nanoparticles. The coating referred to as Aculon throughout this study is Aculon's 'Multi-Surface Hydrophobic Treatment'. It is a nanocoating containing polydimethylsiloxane, a proprietary organometallic component in a hydrocarbon mixture [22]. The fifth coating, Nanopool's Liquid Glass coating [23], the components of which are proprietary, is a transparent hydrophobic nanocoating, designed also to be applied to a wide range of substrates. To facilitate initial characterisation of the coatings, they were applied onto 425 – 550 µm silicon wafer substrates (Pi-Ken ltd). The coatings were later applied onto 25 × 25 x 2 mm, 6 ply +/- 90°, carbon-fibre epoxy composite, manufactured and cut by Juno Composites. The coatings were applied as per manufacturer's instructions, listed in Table 1.

Table 1: Hydrophobic and superhydrophobic coatings with listed components and application method.

Coating	**Components (as per SDS)**	**Application Method**
NeverWet	*Base layer:* polypropylene, methyl isobutyl ketone, butyl acetate and mineral spirits *Top layer:* siloxane derived nano-particles suspended in liquefied petroleum distillates	2 step aerosol - at a fixed height of 25 cm
HydroBead	>90% aliphatic petroleum distillates <10% proprietary additives	1 step aerosol - at a fixed height of 25 cm
SHC	Proprietary additives suspended in an ethanol/methanol mixture	Dip coated - 150 mm / minute
Aculon	Polydimethylsiloxane & proprietary organometallic component in a hydrocarbon mixture	Dip coated - 150 mm / minute
LiquidGlass	N / A	Buffing technique applied by manufacturer

2.2 Plasma pre-treatments

The plasma treatments used in this study were carried out using an air atmospheric pressure plasma jet source called PlasmaTreat™, manufactured by PlasmaTreat GmbH [34]. This jet source consists of two co-axial electrodes, through which the air feed gas is passed through and ionised. Plasma activation was used to treat the composite surface prior to coating; the speed of the jet over the composite was maintained at 30 mm / minute, the nozzle to substrate distance of 15 mm, the 23 kHz discharge used 50% PCT and 90% voltage. The second pre-treatment involved the deposition of an SiO_x interlayer,

using a liquid precursor delivery system called the PlasmaPlus. An SiO_x rich interlayer was deposited using this air plasma source from a Tetraethylorthosilicate (TEOS) precursor. This was passed into the plasma using nitrogen as the carrier gas [35]. The PlasmaTreat processing parameters applied were 80% voltage, 25% PCT and 23 kHz.

2.3 Coating characterisation

The coatings were characterised in terms of physical and chemical properties. The wettability, surface energy, thickness, roughness, morphology and chemical composition were evaluated. The contact angles were measured at room temperature using an OCA 20 system, from Dataphysics Instruments. The sessile drop technique was employed using both static and dynamic measurements. The static measurements were made with 1 µl of deionised water and the dynamic measurements started with a volume of 2 µl, the volume was increased to 10 µl, while recording the advancing angle and reduced to 2 µl while recording the receding angle. The surface energy was obtained using deionised water, diiodomethane and ethylene glycol as test liquids. The Owens, Wendt, Rabel and Kaelble method (OWRK) was used to determine the surface energies [36]. The coating thickness of the non-aerosol coatings was measured using an M-2000® variable angle spectroscopic ellipsometer from J. A. Woollam Co. Measurements, in triplicate at incident angles of 65, 70 and 75°. Analysis of spectroscopic data was carried out using CompleteEase™ analysis software. The coating thickness of the aerosol applied coatings, NeverWet and HydroBead, was obtained on silicon wafer substrates, using step-height difference measurement, measured using a Wyko NT1100 optical profilometer, operating in vertical scanning interferometry (VSI) mode. The arithmetic mean surface roughness (R_a) was determined using the same system. In order to investigate the chemical properties of the coatings, attenuated total reflection infrared spectroscopy (ATR-FTIR) and x-ray photoelectron spectroscopy (XPS) were carried out. The FTIR spectra of the coatings as received in solution, were obtained using a Nicolet iS50 FTIR Spectrometer, Wavenumber range: 8000–650 cm^{-1}, diamond ATR. The atomic concentration of each coating was obtained by X-ray photoelectron spectroscopy (XPS), using a Kratos Analytical Axis Ultra photoelectron spectrometer. A VHX- 5000 Keyence Microscope and an SEM (FEI Quanta 3D Dual Beam FIB) were used to examine the morphology of the coatings.

2.4 Coating durability

The durability of the coatings, when applied on to the carbon-fibre epoxy composite, was investigated using salt spray and abrasion tests. The salt spray test was performed in a salt spray test chamber

following the conditions set in the standard ASTM B-177 [37], The temperature of the chamber was maintained at 35 ºC ± 2 ºC during the test. The 5% NaCl salt solution was fed from an external reservoir into the chamber and the samples were left in the Ascott S450 salt spray chamber for 120 hours. The coatings were monitored in terms of wettability / water contact angle (WCA) as well as the optical examination of the coatings before and after the test was carried out.

A comparative ultrasonic jet abrasion test was used to examine the abrasion resistance of the coated carbon fibre epoxy composite, according to the procedure described by Nwankire et al. [38]. The test involved mounting the coated composites (25 × 25 × 2 mm) onto a sheet of PET and placing it into a 500 ml beaker containing an aqueous slurry of 20 wt % silicon carbide particles (F-60) and deionised water. Into this mixture a UP200H ultrasonic probe (Hielscher Ultrasonics GmbH. Germany), was lowered to 15 mm from the base. The 200 W, 24 kHz ultrasonic probe was set to 100% amplitude and 50% pulsed cycle to agitate the particles and create an abrasive environment. The abrasion resistance test was set up in an SB3-16 sound protection box. At set time intervals, the sheet of PET was removed, the samples were washed with deionised water and dried. The WCA of the samples was then recorded across the centre of the coated substrate in triplicate and re-immersed to continue the abrasion test.

2.5 Protective performance

The protective performance of the coatings was evaluated based on an immersion study in water. The coated and uncoated composite samples were conditioned in deionised water at 50℃, according to the standard D5229/D5229M [39] and the percentage moisture uptake (M) was gravimetrically monitored and recorded as a function of time, according to Eq. 1.

$$M,(\%) = \frac{Wi - Wo}{Wo} \times 100 \qquad \text{Eq. 1}$$

Where W_i is the weight of the conditioned composite at a given time and W_o is the initial weight of the dried specimen. Following this, the coated conditioned composite test specimens were dried in an oven at 50°C for 24 hours. Mechanical testing of composites with and without water immersion was carried out based on interlaminar shear strength (ILSS) testing, as outlined in ASTM D2344 [40]. This involved the use of a three-point bend loading. The mechanical test was carried out using a Tinius-Olsen (US) Hounsfield 50 K screw-driven tensile test machine at room temperature at a speed of 1 mm / min using a 10 kN load cell. Each coating type had a sample set of 10, and the ILSS was calculated according to

equation 2, where F^{sbs} is the short beam strength in MPa, P_m is the maximum load, b is the width and h is the thickness of the specimen.

$$F^{sbs} = 0.75 \times \frac{P_m}{b \times h} \quad \text{Eq. 2}$$

3. Results and Discussion

This section firstly provides the results of the physical and chemical characterisation of the five coatings investigated. Secondly, the coatings are compared in terms of durability and ranked. In order to enhance the bonding performance of the coatings, the use of an air plasma jet, operating at atmospheric pressure for epoxy activation, as well as for the application of an SiO_x interlayer, prior to the application of the hydrophobic coatings, is investigated. Finally, the percentage water ingress and the interlaminar shear properties of the coated composite specimens is compared to examine the barrier performance of the coatings.

3.1 Characterisation

The five coatings, NeverWet, HydroBead, SHC, Aculon and LiquidGlass were evaluated based on their water contact angle, surface energy, thickness, roughness and chemical composition. Hydrophobicity is determined by the water contact angle (WCA). Values of < 90° are typically described as hydrophilic, WCA > 90° hydrophobic and WCA > 150° as superhydrophobic [41]. This is often measured using the static sessile drop technique. To obtain measurements on a superhydrophobic surface, an increase in the droplet volume is often necessary, leading to a deformation of the droplet, causing error of the true result [42]. To overcome this, the contact angle hysteresis was used, which is the difference between the advancing (θ_A) and receding angles (θ_R) [43]. Table 2 details the advancing and receding angles, with their corresponding hysteresis. The NeverWet and HydroBead coatings are characterised as superhydrophobic, as their CAH < 10°, SHC is near superhydrophobic (CAH = 13°) and Aculon and LiquidGlass are hydrophobic.

The surface energy and the roughness of a surface are the dominant factors for wettability [44]. Table 2 details the surface energies of the five coatings, broken down into their polar and dispersive components alongside their average roughness values, expressed as R_a. The NeverWet and SHC coatings were found

to have high surface energies for superhydrophobic coatings, which are typically in the range of 5 – 10 mJ/m² as seen with HydroBead and this is attributed to the high polar content of the two coatings. The high polarity is a result of the high concentration of oxygen, observed in the XPS analysis of both coatings, as seen in Figure 1. All five coatings are primarily composed of Si, C and O, with LiquidGlass being the only coating to have fluorine functionality.

Table 2: Characterisation of coatings on polished silicon wafer. (WCA: water contact angle, θ_A: advancing angle, θ_R: receding angle, CAH: contact angle hysteresis, SE: surface energy, R^a: roughness)

Coating	**WCA (°)**			**SE mJ/m²**	**Disp. (%)**	**Polar (%)**	**Thickness (nm)**	**R_a (nm)**
	θ_A	**θ_R**	**CAH**					
NeverWet	154 ± 2	146 ± 1	8	42	67	33	6.7 ± 0.1 µm	6.2 ± 0.3 µm
HydroBead	159 ± 1	152 ± 1	7	8	75	25	384 ± 80	201 ± 18
SHC	162 ± 3	149 ± 1	13	45	64	36	110 ± 34	27 ± 5
Aculon	110 ± 1	96 ± 1	14	21	100	0	68 ± 10	27 ± 4
LiquidGlass	108 ± 2	85 ± 3	23	13	85	15	11 ± 0.2	2 ± 0.1

As detailed in Table 2, there are considerable differences between these commercial coatings. Firstly, they range from 11 nm to 6 µm in thickness. This is partly due to the method of deposition, for example more material is applied during spray deposition compared with dipping. Factors which have been shown to influence the water repelling mechanism include the surface energy and roughness [44]. Comparing the water contact angles obtained with those reported in the literature for some of these coatings, the values reported for NeverWet[24-27, 45-47] , a static WCA ranging between 143 - 165°, a contact angle hysteresis in the range of 2 - 8° and a roughness between 2 – 6 µm compare well with the obtained values in this study. A WCA of 149 – 166 ° and a contact hysteresis was reported for HydroBead[25, 46, 48] and a static contact angle of 111° reported for Aculon [49] are also within range of those obtained in this study.

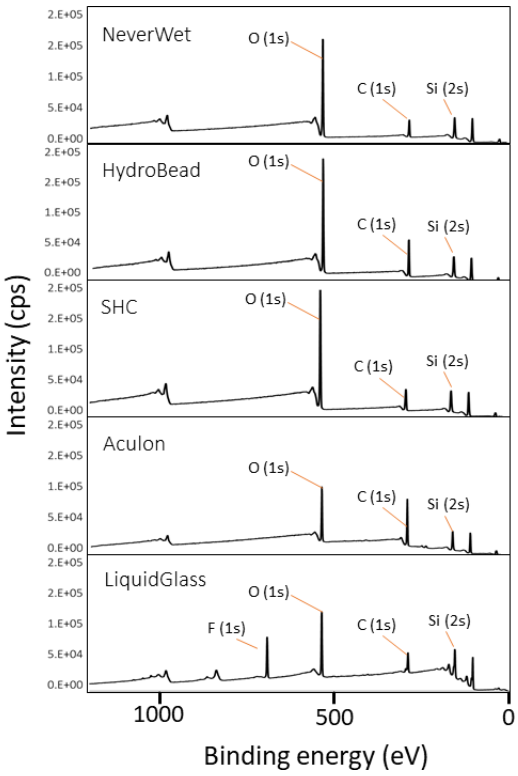

Figure 1: Binding energies from the XPS survey scans of the NeverWet, HydroBead, SHC, Aculon and the LiquidGlass coatings.

Figure 2 gives the ATR FT-IR spectra of the Aculon, HydroBead, SHC, NeverWet base and NeverWet top coat, analysed in solution, as received from manufacturer. The Aculon spectrum exhibits peaks typical of PDMS at 789–796 cm^{-1} (CH_3 rocking and Si-C stretching in Si-CH_3), 1020–1076 cm^{-1} (Si-O-Si stretching), 1260 cm^{-1} (CH_3 deformation in Si-CH_3), and 2950–2960 cm^{-1} (CH_3 stretching in Si-CH_3) [50]. Considerably less functionality was observed in for the spray solution with HydroBead as shown in spectrum 2. Only peaks which could be attributed to the presence of a hydrocarbon solvent were obtained i.e. at 1445 cm^{-1} (C-H bending) and 2810 – 2910 cm^{-1} (C-H stretching) frequencies. The IR peaks obtained for the SHC solution are attributed to siloxane immersed in an alcohol solution; 950 cm^{-1} (O-H bending), 1018–1075 cm^{-1} (Si-O-Si stretching), 1190, 1420 cm^{-1} (O-H bend) , 2800 – 2971 cm^{-1} (C-H stretching) and 3340 cm^{-1} (O-H stretch) [50, 51]. The IR spectrum obtained for the NeverWet base coating exhibited peaks characteristic of both methyl isobutyl ketone, at 1242 cm^{-1} (C-OH stretch), 1370 cm^{-1} (CH_2 bending), 1720 cm^{-1} (C=O), 2875, 2960 cm^{-1} (CH_3 stretching) and of polypropylene at 997 cm^{-1} (CH_3 rock, CH_3 bend), 1166 (C-H bend, CH_3 rock) [52]. The last spectra, for the NeverWet topcoat exhibits peaks at 1200 cm^{-1} (C-OH stretch), 1350, 1420 cm^{-1} (CH_3 bend) and 1700 cm^{-1} (C=O stretch).

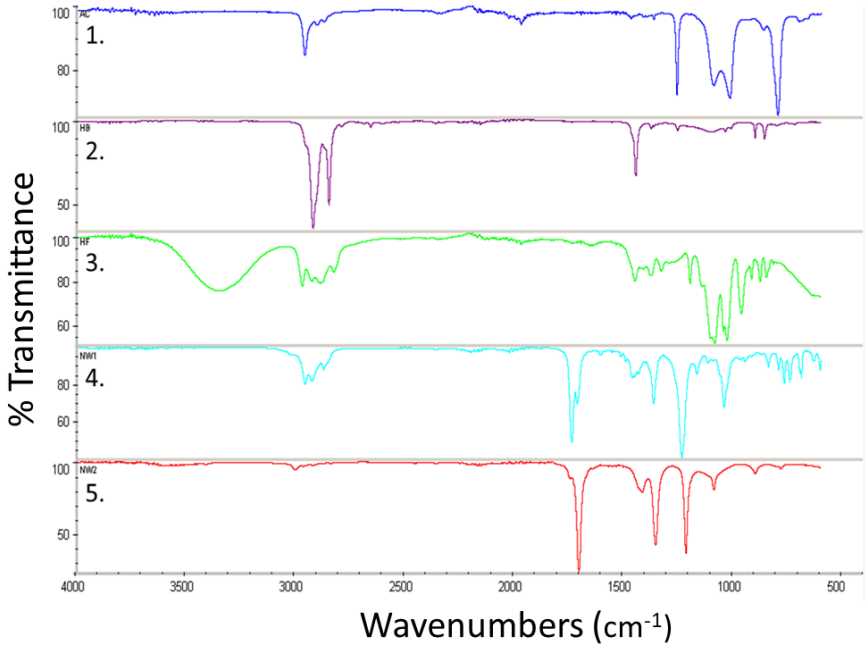

Figure 2: ATR-FTIR spectra of 1. Aculon, 2. HydroBead, 3. SHC, 4. NeverWet base, 5. NeverWet topcoat.

SEM images obtained on the morphology of the five coatings deposited on silicon wafer substrates is illustrated in Figure 3. All of the coatings, except the LiquidGlass coating, exhibit a rough, porous exterior with randomised clusters of nanoparticles. Figure 4 gives an image of the carbon-fibre epoxy substrate coated with HydroBead coating, alongside a roughness plot and a static water contact angle for HydroBead.

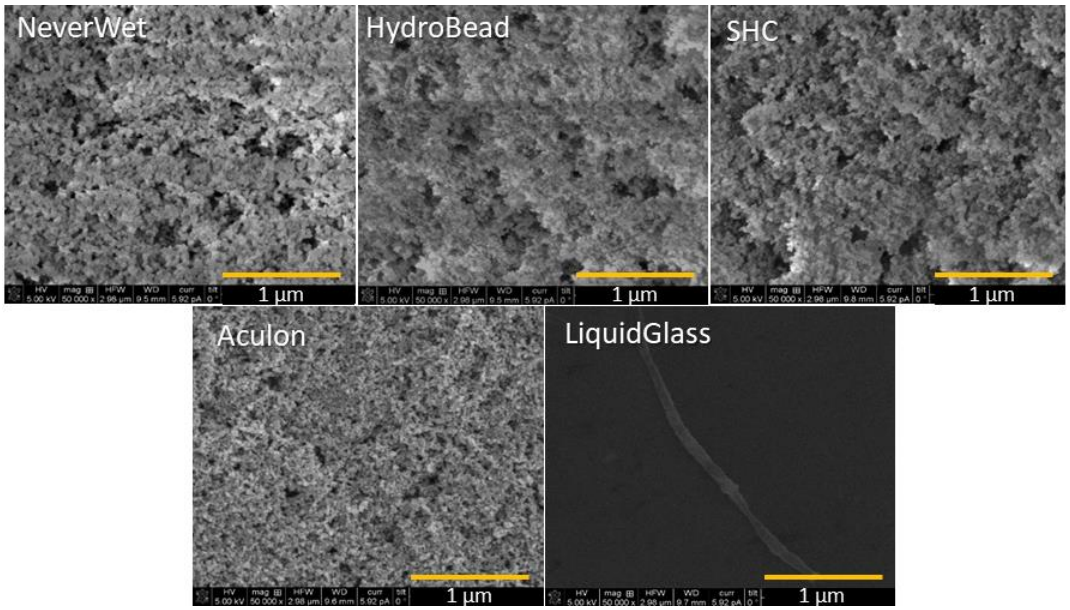

Figure 3: Micrographs of the morphology of NeverWet, HydroBead, SHC, Aculon and the LiquidGlass coatings, deposited on a silicon wafer.

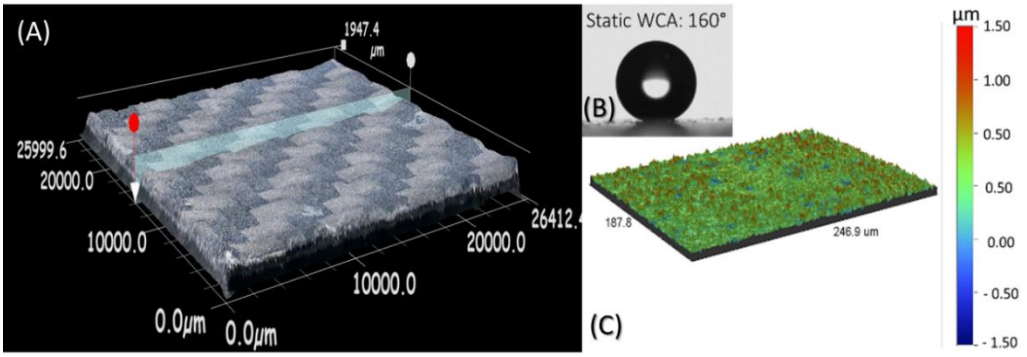

Figure 4: *(A)* Carbon-fibre epoxy specimen coated with HydroBead, *(B)* Static water contact droplet on HydroBead, *(C)* Profilometry roughness plot of HydroBead.

3.2 Coating durability

The wide spread implementation of superhydrophobic coatings has been limited, due to the need for resistance to physical abrasion, erosion, chemical exposure, high temperatures and ultraviolet radiation [53, 54] . In this study, the durability of the coatings is evaluated based on a salt spray and abrasion test. The adhesion performance of the coatings after salt spray testing was assessed based on both optical microscopy examination as well as changes in water contact angle. The latter is demonstrated in Figure 5. After removal from the salt spray chamber and washed with deionised water, the NeverWet and SHC coatings were found to maintain their superhydrophobicity, while the other coatings exhibited some reduction. This was particularly the case for the HydroBead coating, with a decrease of 45° in WCA, which was associated with the partial delamination of the coating, observed using optical microscopy. No signs of delamination were observed for the other coatings.

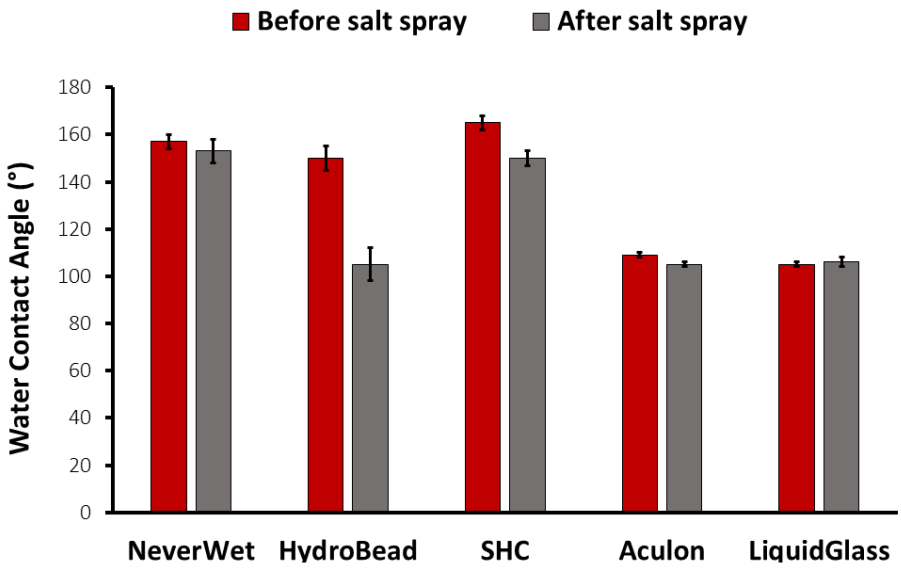

Figure 5: Static water contact angle of hydrophobic coatings before and after 120 hours in salt spray test

A pulsed sonicated, aqueous silicon carbide abrasion test was set up to compare the abrasion resistance of the coatings. The decrease in WCA, at set time intervals, was used as a measure of abrasion resistance. Figure 6 compares the abrasion resistance of the five coatings, in terms of loss of WCA. The coatings, without any pre-treatment, were ranked in the following order alongside their percentage loss of WCA: NeverWet (34%) > Aculon (40%) > HydroBead (59%) > SHC (82%) > LiquidGlass (100%). As expected, the thickness of the coating clearly has a significant role on abrasion resistance performance, as the coating with the highest thickness, NeverWet had the least amount of abrasion and the thinnest coating was completely removed. While NeverWet, without the use of additional pre-treatments, exhibits the highest abrasion resistance of the five coatings evaluated in this study, it is important to note its low abrasion resistance in comparison to non-commercial superhydrophobic coatings being developed [30, 55]. These recent publications from Peng et al. [57] and Huang et al. [31], show that superior durability can be achieved when the coatings are multi-layered and multi-functional, meaning each level of the coating exhibits intrinsic hydrophobicity as the layers are removed, through the use of fluorinated and silica nanoparticles.

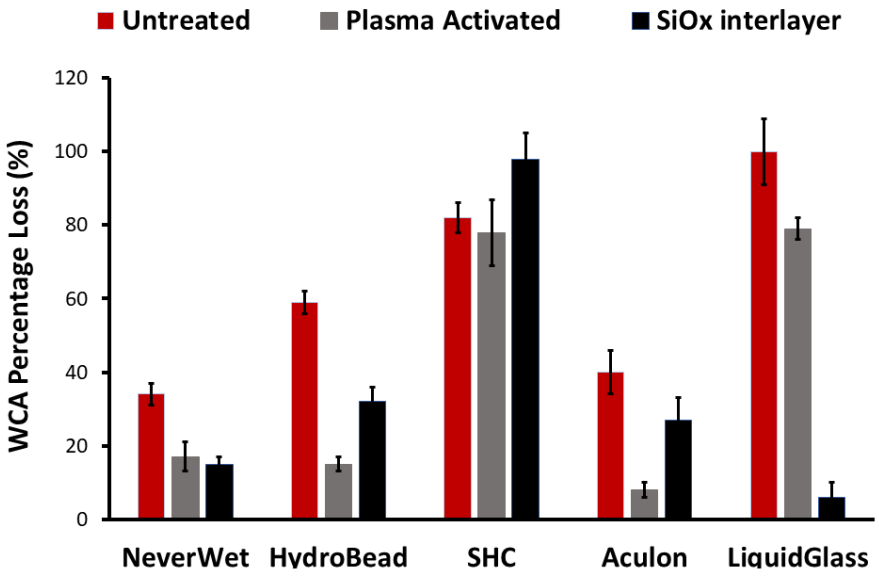

Figure 6: The abrasion resistance of the coatings and the plasma pre-treatments, expressed in terms of percentage loss of WCA.

In order to enhance the abrasion resistance of the commercial coatings, two atmospheric plasma pre-treatments were investigated by increasing the wettability of the composite substrate, prior to coating. The first is the activation of the epoxy composite, using the atmospheric pressure plasma jet, as described in section 2.2. This method of plasma activation has been widely studied and leads to the formation of hydrophilic C-O and C=O on the epoxy surface, increasing the polarity and surface free energy and in turn enhancing the bonding performance of adhesives and coatings on the composite substrate [56, 57]. The second pre-treatment was a silicon oxide interlayer, deposited using the same plasma source by plasma polymerising a TEOS precursor in an oxidising environment. The coating was deposited as described in section 2 and resulted in a silicon oxide layer with an average thickness of 160 nm and an average roughness (R_a) of 2.4 nm, as deposited on to a polished silicon wafer. The wettability of the epoxy composite as received, activated and with the SiO_x interlayer is given in Table 3. In both cases, the pre-treatments increased the surface energy.

Table 3: Surface energies of the epoxy composite surface, before and after plasma pre-treatments

	WCA (°)	**SE (mJ/ m²)**	**Disp. (mJ/m²)**	**Polar (mJ/m²)**
CF / Epoxy	89 ± 1.1	35.9	34.4	1.5
Activated CF / Epoxy	31 ± 1.2	64.1	40.6	23.4
SiO_x interlayer	31 ± 0.8	57.6	36.2	21.4

Figure 6 compares the abrasion resistance of the coatings, as a percentage of the water contact angle loss. The application of the both pre-treatments prior to coating, resulted in enhanced abrasion resistance for NeverWet, HydroBead, Aculon and LiquidGlass. The plasma pre-treatments were not found to effect on the abrasion resistance of the SHC coating, which exhibited extremely poor adhesion with and without pre-treatments. The LiquidGlass and SiO_x interlayer combination exhibited the highest abrasion resistance. This is due to the fluorine content in the LiquidGlass, making it the most durable coating once its thickness was increased.

3.4 Immersion testing

Previous studies have reported poor adhesion of the NeverWet coating [30, 55], however, there have been no reports on the barrier performance of these hybrid commercial coatings. In this study, the protective performance of the coatings was evaluated by immersing the coated composite in deionised water, according to ASTM - D5229 and gravimetrically monitoring the moisture uptake in fibre-polymeric composites. Water absorption in fibre reinforced polymer composites is typically a two-stage process, rapid ingress occurs at the initial stage, followed by a later stage where the absorption levels off and the composite approaches saturation [58]. This is referred to as Fickian diffusion behaviour. Non-Fickian behaviour may also be observed, where the water absorption curve represents a two stage or sigmoidal graph [58]. Figure 7 compares the rate of water ingress as a function of the square root of time for the best performing coating, Aculon and the worst, NeverWet, in terms of barrier performance. All five coatings exhibit moisture diffusion in a two stage, non-Fickian manner. Table 4 details the percentage moisture uptake for each of the coated and uncoated composite specimens. The composite coated with the Aculon, HydroBead and LiquidGlass coatings absorb 13%, 13% and 8% less than the uncoated composite, respectively. While the plasma pre-treatments achieved enhanced adhesion of the coatings, they appear to offer no enhanced barrier performance.

Table 4: Percentage moisture ingress of the coated composites.

	Coating only	**Activated / coating**	**SiOx + coating**	**Uncoated composite**
NeverWet	1.05 ± 0.02	1.15 ± 0.14	0.99 ± 0.06	1.08 ± 0.12
HydroBead	0.94 ± 0.02	1.00 ± 0.05	1.21 ± 0.08	
SHC	1.00 ± 0.12	0.95 ± 0.04	1.02 ± 0.25	
Aculon	0.94 ± 0.03	1.01 ± 0.12	0.90 ± 0.04	
LiquidGlass	0.99 ± 0.03	0.99 ± 0.05	1.02 ± 0.02	

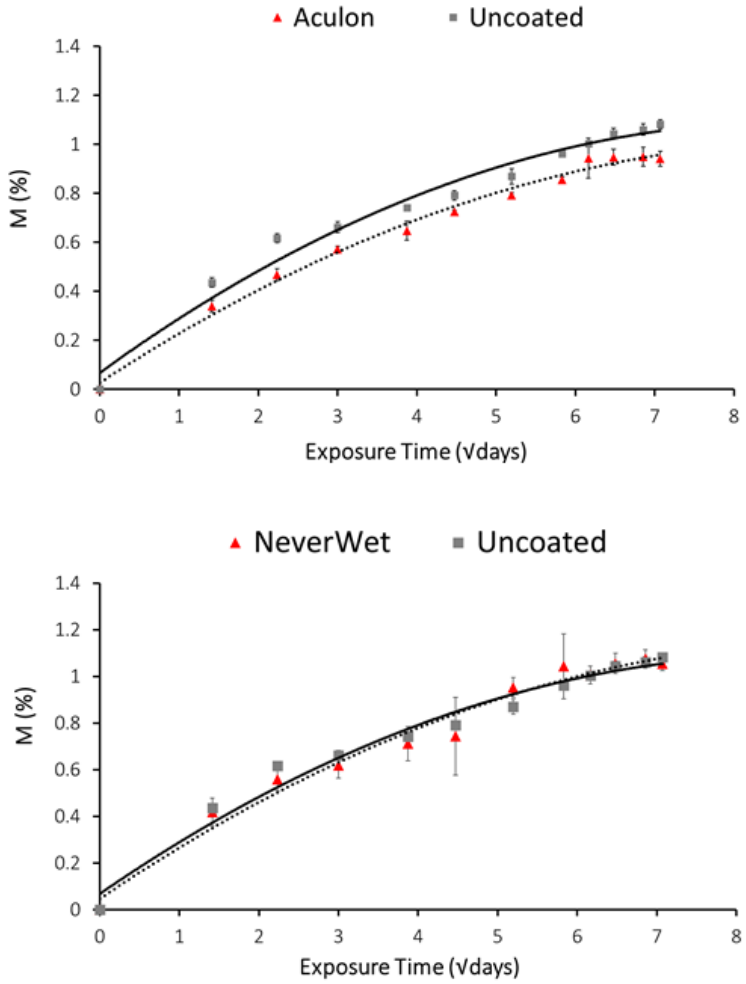

Figure 7: The percentage moisture ingress of the Aculon coated specimen *(top)*, and the NeverWet coating *(bottom)* as a function of the square root of time. The solid line depicts the uncoated specimen and the dashed lines represent the coating.

3.5 Mechanical strength

The effects of water ingress on FRP composites has been well documented [59-64] and is known to cause matrix plasticization and micro-cracking, which in turn can weaken the fibre-matrix interface. As the shear properties of composites are strongly influenced by the strength of the fibre-matrix interface [65], a short beam shear test was used to evaluate if the water ingress in this study lead to irreversible damage and could be used as a measure of coating performance. Once the immersion study was complete, the specimens were dried in an oven at 50°C for 5 days and then their interlaminar shear strength (ILSS) tested.

Table 5 compares the ILSS of the coated and uncoated composite after immersion testing. The ILS strength of the composite as received is 48 ± 3 MPa and the uncoated composite specimen, dried after the immersion test, had an ILSS of 36 ± 2 MPa. The ILSS for the five test coatings was in the order:

LiquidGlass > NeverWet > Aculon > SHC > HydroBead

These values which were 34, 30, 22, 17 and 13%, respectively higher than the uncoated composite, after immersion testing. As previously mentioned, plasticization of the epoxy matrix due to moisture ingress is reversible upon moisture desorption, while hydrolysis of chemical bonds results in more permanent irreversible damage to the epoxy [5]. In the case of the composite substrate coated with LiquidGlass, NeverWet and activated and coated with Aculon, no damage to the carbon-epoxy interface was observed. While the coatings did not prevent moisture ingress - according to the gravimetrical study, it is proposed that they inhibited and altered the route and depth of the moisture. The failure mode exhibited by the LiquidGlass coated composite was a combination of interlaminar shear and inelastic deformation (Figure 8). In contrast, for the composites coated with the other hydrophobic coatings, the failure modes were dominated by inelastic deformation.

Table 5: A comparison of interlaminar shear strength of uncoated and coated and carbon-fibre epoxy.

Specimen	**No Pre-treatment**	**Activation**	**SiO_x Interlayer**
As received	47.9 ± 2.9	-	-
NeverWet	46.9 ± 3.8	46.2 ± 2.8	44.6 ± 8.9
HydroBead	40.8 ± 6.0	41.6 ± 3.2	45.6 ± 5.7
SHC	42.0 ± 5.9	42.6 ± 4.0	42.8 ± 82
Aculon	43.9 ± 6.1	47.2 ± 3.9	41.3 ± 8.5
LiquidGlass	48.3 ± 4.7	39.3 ± 5.6	39.2 ± 6.5
Uncoated	35.9 ± 2.4	-	-

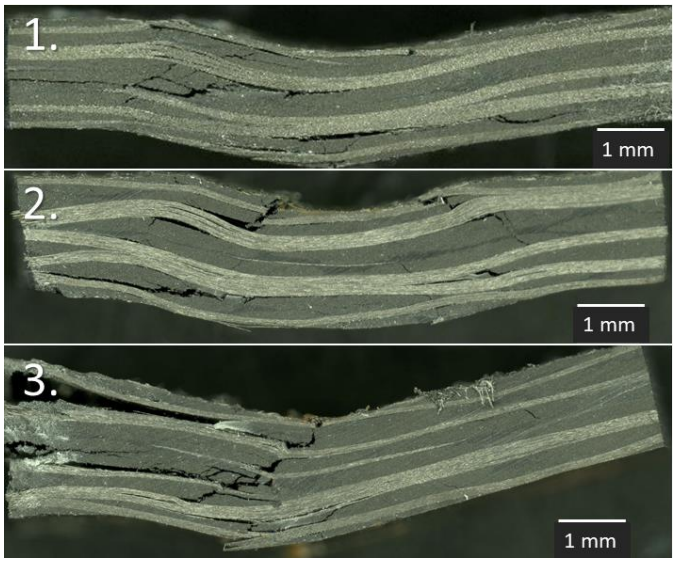

Figure 8: Observed failure modes of 1. LiquidGlass coated composite, 2. Uncoated composite and 3. Uncoated untested composite (as received).

4 Conclusions

The aim of this study was to investigate the performance of five commercial coatings to protect carbon-fibre epoxy composite against abrasion and water ingress. The coatings were characterised in terms of roughness, thickness, chemical composition and morphology. It is concluded that the NeverWet, HydroBead owe their hydrophobicity to their relatively high surface roughness, while the LiquidGlass to its fluorine chemistry (14%). Based on the salt spray fog and abrasion tests, the durability of the coatings, prior to the application of plasma pre-treatments, was ranked in the following order; NeverWet > Aculon > HydroBead > SHC > LiquidGlass.

Thickness plays a considerable role in this ranking, with the NeverWet being by far the thickest of the layers at 6673 nm. The Aculon layer also performed very well, despite it being the second thinnest coating at 68 nm. To over come poor coating adhesion, previously reported in the literature for the NeverWet coating, two atmospheric pressure plasma pre-treatments were evaluated. Both the use of plasma activation and the deposition of the SiO_x nanocoating significantly increased the wettability of the epoxy composite substrate. In turn, this significantly enhanced the abrasion resistance for the NeverWet, HydroBead, Aculon and LiquidGlass coatings.

The protective performance of the coatings was evaluated based on a water immersion testing, followed by mechanical testing of the coated composite coupons. The application of the Aculon, HydroBead and LiquidGlass coating resulted in a 13, 13 and 8% reduction in water absorption when compared to the uncoated composite. The interlaminar shear properties of the coated and uncoated composite were

evaluated after immersion testing, on the dried specimens, facilitating the investigation of irreversible damage to the fibre-matrix interface. LiquidGlass, NeverWet, Aculon, SHC and HydroBead coated specimens exhibited an increase in ILSS of 34, 30, 22, 17 and 13% compared with that obtained for the uncoated composite. Upon moisture desorption, the LiquidGlass, NeverWet coated parts, and plasma pre-treated / Aculon coated composite exhibited no loss in interlaminar strength.

It is concluded from this study that:

- The commercial coatings exhibit a rough nano-structured morphology and are fluorine free, except for the LiquidGlass coating, which exhibited extremely low roughness and fluorine content.
- Plasma activation and the deposition of an SiO_x interlayer both increased the surface energy of the composite substrate and lead to enhanced abrasion performance of four of the commercial coatings.
- The Aculon coating and LiquidGlass in combination with an SiO_x interlayer, exhibit the greatest potential to be further developed as a protective coating for use in conjunction with carbon-fibre epoxy composites.

Declaration of conflicting Interests

The authors declared no potential conflicts of interest with respect to the research, authorship and / or publication of this article.

Acknowledgements

This work was supported under both the SFI funded I-Form Advanced Manufacturing Research Centre – (16/RC/3872), and the MaREI SFI Centre for Marine Renewable Energy Research - (12/RC/2302).

References

1. Harris B. *Composite Materials* The Institute of Materials, London 1999.
2. Zafar A, Bertocco F, Schjødt-Thomsen J, et al. Investigation of the long term effects of moisture on carbon fibre and epoxy matrix composites. *Composites Science and Technology* 2012; 72: 656-666. DOI: 10.1016/j.compscitech.2012.01.010.
3. Lubineau G and Rahaman A. A review of strategies for improving the degradation properties of laminated continuous-fiber/epoxy composites with carbon-based nanoreinforcements. *Carbon* 2012; 50: 2377-2395. DOI: 10.1016/j.carbon.2012.01.059.

4. Almeida JHS, Souza SDB, Botelho EC, et al. Carbon fiber-reinforced epoxy filament-wound composite laminates exposed to hygrothermal conditioning. *Journal of Materials Science* 2016; 51: 4697-4708. DOI: 10.1007/s10853-016-9787-9.
5. Bhavesh G. Kumar RPS, Toshio Nakamura Degradation of Carbon Fiber-reinforced Epoxy Composites by Ultraviolet Radiation and Condensation. *Journal of Composite Materials* 2002; 36: 2713 - 2733. DOI: 10.1106/002199802028682.
6. Shen C-H, Springer, George S. Moisture Absorption and Desorption of Composite Materials. *Journal of Composite Materials* 2016; 10: 2-20. DOI: 10.1177/002199837601000101.
7. H.S. Choi KJA, J.D. Nam, H.J. Chun. Hygroscopic aspects of epoxy/carbon fiber composite laminates in aircraft environments. *Composites Part A: Applied Science and Manufacturing* 2001; 32: 709 - 720.
8. Layton J. Weathering. In: Pritchard G (ed) *Reinforced Plastics Durability*. Woodhead Publishing, 1999, pp.186 - 216.
9. Tracton AA. *Coatings Technology Handbook*. 3rd ed.: Taylor & Francis, 2005.
10. Hughes JF. Electrostatic powder coating. *Encyclopedia of Physical Science and Technology* 2002: 379-391.
11. LeBlanc J, Gardner N and Shukla A. Effect of polyurea coatings on the response of curved E-Glass/Vinyl ester composite panels to underwater explosive loading. *Composites Part B: Engineering* 2013; 44: 565-574. DOI: 10.1016/j.compositesb.2012.02.038.
12. Scholz S, Kroll L and Schettler F. Nanoparticle reinforced epoxy gelcoats for fiber-plastic composites under multiple load. *Progress in Organic Coatings* 2014; 77: 1129-1136. DOI: 10.1016/j.porgcoat.2014.03.012.
13. Wang Y, Lim S, Luo JL, et al. Tribological and corrosion behaviors of Al2O3/polymer nanocomposite coatings. *Wear* 2006; 260: 976-983. DOI: https://doi.org/10.1016/j.wear.2005.06.013.
14. See SC, Zhang ZY and Richardson MOW. A study of water absorption characteristics of a novel nano-gelcoat for marine application. *Progress in Organic Coatings* 2009; 65: 169-174. DOI: 10.1016/j.porgcoat.2008.11.004.
15. Shi H, Liu F, Yang L, et al. Characterization of protective performance of epoxy reinforced with nanometer-sized TiO2 and SiO2. *Progress in Organic Coatings* 2008; 62: 359-368. DOI: https://doi.org/10.1016/j.porgcoat.2007.11.003.
16. Nosonovsky M and Bhushan B. Superhydrophobic surfaces and emerging applications: Non-adhesion, energy, green engineering. *Current Opinion in Colloid & Interface Science* 2009; 14: 270-280. DOI: 10.1016/j.cocis.2009.05.004.
17. Bhushan B and Jung YC. Natural and biomimetic artificial surfaces for superhydrophobicity, self-cleaning, low adhesion, and drag reduction. *Progress in Materials Science* 2011; 56: 1-108. DOI: 10.1016/j.pmatsci.2010.04.003.
18. Antonini C, Innocenti M, Horn T, et al. Understanding the effect of superhydrophobic coatings on energy reduction in anti-icing systems. *Cold Regions Science and Technology* 2011; 67: 58-67. DOI: 10.1016/j.coldregions.2011.02.006.
19. Luo SC, Liour SS and Yu HH. Perfluoro-functionalized PEDOT films with controlled morphology as superhydrophobic coatings and biointerfaces with enhanced cell adhesion. *Chem Commun (Camb)* 2010; 46: 4731-4733. DOI: 10.1039/c002321c.

20. NeverWet Product Website, http://www.neverwet.com/, (2017, accessed 12/04/2017 2017).
21. HydroBead, http://www.hydrobead.com/ (accessed 10/12/17 2017).
22. Aculon Performance Surface Solution, http://www.aculon.com/, (2017, accessed 1/12/17 2017).
23. Nanopool Product: npLiquidGlass http://npliquidglass.ie/, (accessed 12/04/17 2017).
24. Gupta R, Vaikuntanathan V and Sivakumar D. Superhydrophobic qualities of an aluminum surface coated with hydrophobic solution NeverWet. *Colloids and Surfaces A: Physicochemical and Engineering Aspects* 2016; 500: 45-53. DOI: 10.1016/j.colsurfa.2016.04.017.
25. Rajaram M, Heng X, Oza M, et al. Enhancement of fog-collection efficiency of a Raschel mesh using surface coatings and local geometric changes. *Colloids and Surfaces A: Physicochemical and Engineering Aspects* 2016; 508: 218-229. DOI: 10.1016/j.colsurfa.2016.08.034.
26. Lai CQ, Chia Wei Shen J, Chua Wei Cheng W, et al. A near-superhydrophobic surface reduces hemolysis of blood flow in tubes. *RSC Adv* 2016; 6: 62451-62459. DOI: 10.1039/c6ra12376g.
27. Ramachandran R and Nosonovsky M. Coupling of surface energy with electric potential makes superhydrophobic surfaces corrosion-resistant. *Phys Chem Chem Phys* 2015; 17: 24988-24997. DOI: 10.1039/c5cp04462f.
28. Tian X, Shaw S, Lind KR, et al. Thermal Processing of Silicones for Green, Scalable, and Healable Superhydrophobic Coatings. *Adv Mater* 2016; 28: 3677-3682. DOI: 10.1002/adma.201506446.
29. Zhi D, Wang H, Jiang D, et al. Reactive silica nanoparticles turn epoxy coating from hydrophilic to super-robust superhydrophobic. *RSC Advances* 2019; 9: 12547-12554. DOI: 10.1039/c8ra10046b.
30. Huang Z-S, Quan Y-Y, Mao J-J, et al. Multifunctional superhydrophobic composite materials with remarkable mechanochemical robustness, stain repellency, oil-water separation and sound-absorption properties. *Chemical Engineering Journal* 2019; 358: 1610-1619. DOI: 10.1016/j.cej.2018.10.123.
31. Abourayana HM and Dowling DP. Plasma Processing for Tailoring the Surface Properties of Polymers. 2015. DOI: 10.5772/60927.
32. Dowling DP. Surface Processing Using Cold Atmospheric Pressure Plasmas. 2014: 171-185. DOI: 10.1016/b978-0-08-096532-1.00408-8.
33. P.K. Chu, J.Y. Chen, L.P. Wang, et al. Plasma-surface modification of biomaterials *Materials Science and Engineering* 2002; 36: 143-206.
34. Dowling DP, O'Neill FT, Langlais SJ, et al. Influence of dc Pulsed Atmospheric Pressure Plasma Jet Processing Conditions on Polymer Activation. *Plasma Processes and Polymers* 2011; 8: 718-727. DOI: 10.1002/ppap.201000145.
35. Dowling DP and Stallard CP. Achieving enhanced material finishing using cold plasma treatments. *Transactions of the IMF* 2015; 93: 119-125. DOI: 10.1179/0020296715z.000000000240.
36. D. K. Owens RCW. Estimation of the Surface Free Energy of Polymers. *Journal of Applied Polymer Science* 1969; 13: 1741 - 1747. DOI: 10.1002/app.1969.070130815.
37. Standard Practice for Operating Salt Spray (Fog) Apparatus.

38. Nwankire CE, Favaro G, Duong Q-H, et al. Enhancing the Mechanical Properties of Superhydrophobic Atmospheric Pressure Plasma Deposited Siloxane Coatings. *Plasma Processes and Polymers* 2011; 8: 305-315. DOI: 10.1002/ppap.201000069.
39. Standard Test Method for Moisture Absorption Properties and Equilibrium Conditioning of Polymer Matrix Composite Materials.
40. 2344M ADD. Standard Test Method for Short-Beam Strength of Polymer Matrix Composite Materials and Their Laminates. 2000.
41. Celia E, Darmanin T, Taffin de Givenchy E, et al. Recent advances in designing superhydrophobic surfaces. *J Colloid Interface Sci* 2013; 402: 1-18. DOI: 10.1016/j.jcis.2013.03.041.
42. Zhang X, Shi F, Niu J, et al. Superhydrophobic surfaces: from structural control to functional application. *J Mater Chem* 2008; 18: 621-633. DOI: 10.1039/b711226b.
43. McCarthy LGaTJ. Contact Angle Hysteresis Explained. *Langmuir* 2006; 22: 6234 - 6237.
44. Miwa; M, Fujishima; A, Hashimoto; K, et al. Effects of the Surface Roughness on Sliding Angles of Water Droplets on Superhydrophobic Surfaces. *Langmuir* 2000; 16: 5754 - 5760.
45. Kim N, Kim H and Park H. An experimental study on the effects of rough hydrophobic surfaces on the flow around a circular cylinder. *Physics of Fluids* 2015; 27: 085113. DOI: 10.1063/1.4929545.
46. Amirfazli A. Effects of Prolonged Exposure to UV and Water on Super-Hydrophobic Surfaces at Ambient and Icing Conditions. 2015; 1. DOI: 10.4271/2015-01-2160.
47. Waghmare PR, Mitra S, Kumar Gunda NS, et al. Needle-free drop deposition: the role of elastic membranes. *RSC Adv* 2015; 5: 82374-82380. DOI: 10.1039/c5ra15938e.
48. Krishnan KG, Milionis A, Loth E, et al. Influence of hydrophobic and superhydrophobic surfaces on reducing aerodynamic insect residues. *Applied Surface Science* 2017; 392: 723-731. DOI: 10.1016/j.apsusc.2016.09.096.
49. Yeong YH, Milionis A, Loth E, et al. Atmospheric Ice Adhesion on Water-Repellent Coatings: Wetting and Surface Topology Effects. *Langmuir* 2015; 31: 13107-13116. DOI: 10.1021/acs.langmuir.5b02725.
50. Gonzalez-Rivera J, Iglio R, Barillaro G, et al. Structural and Thermoanalytical Characterization of 3D Porous PDMS Foam Materials: The Effect of Impurities Derived from a Sugar Templating Process. *Polymers (Basel)* 2018; 10. DOI: 10.3390/polym10060616.
51. Coldea TE, Socaciu C, Fetea F, et al. Rapid Quantitative Analysis of Ethanol and Prediction of Methanol Content in Traditional Fruit Brandies from Romania, using FTIR Spectroscopy and Chemometrics. *Notulae Botanicae Horti Agrobotanici* 2013; 41: 143-149.
52. Jung MR, Horgen FD, Orski SV, et al. Validation of ATR FT-IR to identify polymers of plastic marine debris, including those ingested by marine organisms. *Mar Pollut Bull* 2018; 127: 704-716. DOI: 10.1016/j.marpolbul.2017.12.061.
53. Zhu X, Zhang Z, Men X, et al. Robust superhydrophobic surfaces with mechanical durability and easy repairability. *Journal of Materials Chemistry* 2011; 21: 15793. DOI: 10.1039/c1jm12513c.

54. Girard H-L, Khan S and Varanasi KK. Multilevel robustness. *Nature Materials* 2018; 17: 298-300. DOI: 10.1038/s41563-018-0051-3.
55. Peng C, Chen Z and Tiwari MK. All-organic superhydrophobic coatings with mechanochemical robustness and liquid impalement resistance. *Nat Mater* 2018; 17: 355-360. DOI: 10.1038/s41563-018-0044-2.
56. Coulon JF, Tournerie N and Maillard H. Adhesion enhancement of Al coatings on carbon/epoxy composite surfaces by atmospheric plasma. *Applied Surface Science* 2013; 283: 843-850. DOI: 10.1016/j.apsusc.2013.07.028.
57. Zaldivar RJ, Nokes J, Steckel GL, et al. The Effect of Atmospheric Plasma Treatment on the Chemistry, Morphology and Resultant Bonding Behavior of a Pan-Based Carbon Fiber-Reinforced Epoxy Composite. *Journal of Composite Materials* 2009; 44: 137-156. DOI: 10.1177/0021998309345343.
58. Dhakal HN, MacMullen J and Zhang ZY. Moisture measurement and effects on properties of marine composites. 2016: 103-124. DOI: 10.1016/b978-1-78242-250-1.00005-3.
59. Kootsookos A and Mouritz AP. Seawater durability of glass- and carbon-polymer composites. *Composites Science and Technology* 2004; 64: 1503-1511. DOI: 10.1016/j.compscitech.2003.10.019.
60. E.P. Gellert DMT. Seawaer immersion ageing of glass-fibre reinforced polymer laminates for marine applications. *Composites: Part A* 1999; 30: 1259 - 1265.
61. Davies P. Environmental degradation of composites for marine structures: new materials and new applications. *Philos T R Soc A* 2016; 374. DOI: ARTN 20150272

10.1098/rsta.2015.0272.
62. Imielińska K and Guillaumat L. The effect of water immersion ageing on low-velocity impact behaviour of woven aramid–glass fibre/epoxy composites. *Composites Science and Technology* 2004; 64: 2271-2278. DOI: 10.1016/j.compscitech.2004.03.002.
63. F. McBagonluri KG, M. Hayes, K.N.E. Verghese, J.J. Lesko. Characterization of fatigue and combined environment on durability performance of glass/vinyl ester composite for infrastructure applications. *International Journal of Fatigue* (2000); 22: 53–64.
64. Akbar S and Zhang T. Moisture Diffusion in Carbon/Epoxy Composite and the Effect of Cyclic Hygrothermal Fluctuations: Characterization by Dynamic Mechanical Analysis (DMA) and Interlaminar Shear Strength (ILSS). *The Journal of Adhesion* 2008; 84: 585-600. DOI: 10.1080/00218460802255434.
65. Khan LA, Nesbitt A and Day RJ. Hygrothermal degradation of 977-2A carbon/epoxy composite laminates cured in autoclave and Quickstep. *Composites Part A: Applied Science and Manufacturing* 2010; 41: 942-953. DOI: 10.1016/j.compositesa.2010.03.003.